Through diffusion experiments to study the diffusion and sorption of HTO, 36Cl, 133Ba and 134Cs in crystalline rock

Aromaa, Hanna

2019-04

Aromaa , H , Voutilainen , M , Ikonen , J , Yli-Kaila , M , Poteri , A & Siitari-Kauppi , M 2019 , ' Through diffusion experiments to study the diffusion and sorption of HTO, 36Cl, 133Ba and 134Cs in crystalline rock ' , Journal of Contaminant Hydrology , vol. 222 , pp. 101-111 . https://doi.org/10.1016/j.jconh

http://hdl.handle.net/10138/301336
https://doi.org/10.1016/j.jconhyd.2019.03.002

Journal of Contaminant Hydrology 222 (2019) 101–111

Contents lists available at ScienceDirect

Journal of Contaminant Hydrology

journal homepage: www.elsevier.com/locate/jconhyd

Through diffusion experiments to study the diffusion and sorption of HTO, ^{36}Cl, ^{133}Ba and ^{134}Cs in crystalline rock

Hanna Aromaa[a], Mikko Voutilainen[a,*], Jussi Ikonen[a], Maarit Yli-Kaila[b], Antti Poteri[b], Marja Siitari-Kauppi[a]

[a] Department of Chemistry, University of Helsinki, P.O. Box 55, 00014, Finland
[b] Posiva Oy, Olkiluoto, Eurajoki 27160, Finland

ARTICLE INFO

Keywords:
Diffusion
Sorption
Porosity
Crystalline rock
Radionuclides
Time-domain random walk

ABSTRACT

The spent nuclear fuel in Finland will be deposited in crystalline granitic rock in Olkiluoto, Finland. As a part of the safety assessment of the repository, series of extensive in-situ sorption and diffusion experiments and supplementary laboratory work has been done in the Olkiluoto site. Through Diffusion Experiment in a laboratory (TDElab) aims to provide applicable data for the ongoing in-situ experiment in Olkiluoto. This laboratory scale experiment resembles the in-situ experiment and aims to gain information on possible effects in values of distribution coefficients, effective diffusion coefficient and porosity that are caused by differences in laboratory and in-situ conditions. The through diffusion and sorption of tracer solution with known activities of HTO, ^{36}Cl, ^{133}Ba and ^{134}Cs were studied in a decimeter scale sample of veined gneiss, which is one of the main rock types in Olkiluoto. The measured breakthrough curves were modeled taking into account the porosity of the rock and diffusion and sorption of the radionuclides using Time-Domain Random Walk (TDRW) simulations. The porosities of 0.7–0.8% were determined for the rock and effective diffusion coefficients of $(3.5 \pm 1.0) \times 10^{-13}$ m^2/s and $(3.0 \pm 1.0) \times 10^{-13}$ m^2/s were determined for HTO and ^{36}Cl, respectively. The porosity and effective diffusion coefficients were found to be in agreement with previous results for veined gneiss. Furthermore, distribution coefficients of $(1.0 \pm 0.3) \times 10^{-4}$ m^3/kg and $(2.0 \pm 0.5) \times 10^{-3}$ m^3/kg were determined for ^{133}Ba and ^{134}Cs, respectively, using information about the effective diffusion coefficient determined for HTO. The distribution coefficients were found to be significantly smaller than the ones determined for crushed rock in previous studies and slightly smaller than the ones from previous in-diffusion experiments.

1. Introduction

The final disposal of spent nuclear fuel (SNF) from present nuclear power plants in Finland (Olkiluoto and Loviisa) is planned to take place in a crystalline granitic rock at Olkiluoto Island (Eurajoki, Finland) (Posiva, 2012). The SNF will be protected by a multiple barrier system. If released into the bedrock, radionuclides will be transported mostly by advection along water conducting fractures. The transport of the radionuclides will be retarded by molecular diffusion from the fractures into the stagnant matrix pore water and/or by sorption onto mineral surfaces in the rock matrix (Neretnieks, 1980; Kekäläinen et al., 2011; Wels et al., 1996). To resolve the magnitude of the retardation, the properties of the bedrock in respect of different radionuclides have to be carefully determined for the safety assessment of the final disposal.

Cesium is a highly soluble alkali metal occurring in the SNF and its inventories in the SNF are among the highest of all radionuclides. ^{135}Cs is one of the critical radionuclides when considering the long-term safety of the final disposal due to its long half-life (Posiva, 2013). This makes the cesium retention properties of the bedrock of great interest in the safety assessment for the final disposal of SNF in deep repositories. In this work, ^{134}Cs was chosen as an analogue for ^{135}Cs. Barium is often used as a chemical analogue for radium which has a radioactive isotope (^{226}Ra) with high importance in the safety assessment of the spent fuel deposition due to the ingrowth from uranium (Nilsson and Papp, 1980). The ^{226}Ra activity will reach a maximum approximately 300,000 years after the deposition of the SNF (Grandia et al., 2008). Understanding the transport properties of barium and radium in the bedrock is of importance for the safety assessment of the repository. Barium and cesium are known to be sorbing elements in the repository conditions and sorb by ion exchange mechanism (Molinero and Samper, 2006; Kyllönen et al., 2014). Furthermore, HTO and ^{36}Cl are commonly used as non-sorbing radionuclides when studying the properties of bedrock

* Corresponding author.
E-mail address: ma.voutilainen@helsinki.fi (M. Voutilainen).

https://doi.org/10.1016/j.jconhyd.2019.03.002
Received 14 December 2018; Received in revised form 13 February 2019; Accepted 8 March 2019
Available online 09 March 2019

(Hou and Roos, 2008) because they represent natural elements in the groundwater (Smellie et al., 2014). They are assumed to not have chemical reaction on the mineral surfaces in granitic rock (Ikonen et al., 2016a). Furthermore, ^{36}Cl has great interest in the safety assessment due to its long half-live and high mobility in the bedrock.

In-situ experiments are important in order to determine the diffusion and distribution coefficient of bedrock in conditions analogous to those at the repository site. However, in-situ experiments are costly and time-consuming. Hence, it is equally important to compare in-situ results with the laboratory experiments to better assess their relevancy. The in-situ diffusion experiments have been performed in several countries e.g. Finland (Poteri et al., 2018; Voutilainen et al., 2014), Sweden (Andersson et al., 2004; Nilsson et al., 2010; Widestrand et al., 2010) and Switzerland (Ikonen et al., 2016a; Soler et al., 2015) to demonstrate the behavior of radionuclides in crystalline bedrock. In Switzerland, the retention of several radionuclides was studied in-situ in Grimsel granodiorite through a long-term diffusion (LTD) experiment (Ikonen et al., 2016a; Soler et al., 2015). Ikonen et al. (2017) reported that the effective diffusion coefficients measured in laboratory and in-situ experiments for Grimsel granodiorite do not differ considerably from each other. On the other hand, Soler et al. (2015) report results from the same experiments that show laboratory effective diffusion coefficients that are a factor of 3 larger than the in-situ coefficients (only results by Japan atomic energy agency are considered here since they are the only group that reports both laboratory and in-situ results). In addition, recent experiments performed in Olkiluoto, Finland, do not show differences between the effective diffusion coefficients determined using the laboratory and in-situ experiments (Poteri et al., 2018). However, the designs of the experimental setups used in the laboratory and in-situ experiments differ in above mentioned studies. Furthermore, in similar in-situ experiment (Long Term Diffusion Experiment, LTDE) the retention of 22 radionuclides was studied at the Äspö Hard Rock Laboratory, Sweden (Nilsson et al., 2010; Widestrand et al., 2010). The focus of LTDE was more directed towards sorption rather than diffusion due to the relatively short experimental time of about six months. The in-diffusion curves have turned out to be rather difficult to explain due to the experimental design and effect of heterogeneity of the rock (Iraola et al., 2017; Park and Ji, 2018).

A project called “rock matrix REtention PROperties” (REPRO) at ONKALO, the underground rock characterization facility in Olkiluoto, Finland consists of extensive series of in-situ sorption and diffusion measurements that are supplemented by laboratory work (Aalto et al., 2009). One of these in-situ experiments is a Through Diffusion Experiment (TDE) launched in the autumn of 2015 for studying the diffusion of HTO, ^{36}Cl, ^{22}Na, ^{133}Ba and ^{134}Cs in the Olkiluoto bedrock (Aromaa et al., 2018). The aim of the REPRO in-situ TDE is to quantify diffusivity and the connected porosity of the unaltered rock matrix in the repository level stress conditions. The experimental setup consists of three parallel drill holes where one is used as an injection hole (decreasing concentrations measured) and the breakthroughs of radionuclides to two observation drill holes are followed (Voutilainen et al., 2014). In this study, the aim has been to perform a replica of the in-situ experiment in the laboratory. The Through Diffusion Experiment in the laboratory (TDElab) aims to study the through diffusion of HTO, ^{36}Cl, ^{133}Ba and ^{134}Cs in veined gneiss sample resembling the Olkiluoto bedrock and provide comparable data for the ongoing in-situ TDE.

Often studies that aim to determine the effective diffusion coefficients and distribution coefficients are performed in the laboratory conditions. Recently such studies have been performed for samples e.g. from Finland (Voutilainen et al., 2016; Muuri et al., 2018), Sweden (Widestrand et al., 2007), Japan (Tachi et al., 2011), Czech Republic (Videnská et al., 2015), Switzerland (Tachi et al., 2015; Muuri et al., 2016) and Canada (Vilks et al., 2003). Typically, the distribution coefficients have been measured using crushed material and batch sorption experiments. However, many of the recent studies show that the crushing increases the specific surface area and sorption capacity of the material which leads to an over-estimation of the distribution coefficients (André et al., 2009; Muuri et al., 2017, 2018; Puukko et al., 2018). To this end, it is important to determine distribution coefficients for intact rock. When performing long term experiments with sorbing nuclides and intact rock, the analysis of the results becomes more complicated since often diffusion has to be taken into account.

One possibility to model such experiments with taking into account the heterogeneity of the rock and other experimental details is to use Time-Domain Random Walk (TDRW) method. The method was originally developed for simulating transport in heterogeneous media (McCarthy, 1993; Delay et al., 2002). The TDRW method is a rapid particle-tracking method where a particle is forced to jump to a neighboring point during a certain random transition time, which makes it faster than the traditional particle-tracking methods (Sardini et al., 2003). The method has been used to study the effect of structural heterogeneities on diffusion in various cases (Sardini et al., 2007; Robinet et al., 2012; Voutilainen et al., 2013). Recently the method has been developed so that it is now possible to take into account sorption applying linear K_d (Dentz et al., 2012; Ikonen et al., 2016b; Voutilainen et al., 2017) and flow in fractured media (Gjetvaj et al., 2015; Noetinger et al., 2016). The method has also been found to be a powerful tool for analyzing the results of both in-situ and laboratory experiments especially when initial or boundary conditions are complicated (Voutilainen et al., 2013; Soler et al., 2015; Ikonen et al., 2017). Due to the recent developments and demonstrated capability to model similar experiments, the TDRW method was chosen as the modeling tool for determining the transport parameters from the measured data.

The aim of TDElab has been to study the diffusion and sorption of HTO, ^{36}Cl, ^{133}Ba and ^{134}Cs and to determine retention parameters (effective diffusion coefficient, porosity and distribution coefficient) for the intact crystalline rock sample from the REPRO site. Later these results can be compared with results from in-situ TDE that is being performed at repository level and with similar experimental design as TDElab. By using a sample geometry resembling the in-situ TDE, one can get comparable information about the effect of experimental conditions on the rock properties. Furthermore, the aim is to produce site specific data for the safety assessment of the repository.

2. Materials and methods

2.1. Rock samples

The Olkiluoto site is situated in south-western Finland on the coast of the Baltic Sea. The REPRO niche where the in-situ experiments are performed is located in 420 m below the surface and the bedrock in the site is pegmatitic granite and migmatitic gneiss (subgroup: veined gneiss). Pegmatitic granite is from light grey to pale colored with coarse K-feldspar and commonly also cordierite and garnet (Pitkänen et al., 1996; Aaltonen et al., 2016). Veined gneiss was chosen for this experiment because it represents the same rock material that surrounds the in-situ TDE bore holes (Sammaljärvi et al., 2017). The veined gneiss shows a weak to moderate banded foliation but locally also irregular foliation. The main minerals of veined gneiss are quartz, plagioclase, biotite and potassium feldspar (Kärki and Paulamäki, 2006). The mineral composition of the bedrock has been shown to be an important factor for the overall sorption properties of the rock (Kuva et al., 2018; Muuri et al., 2016; Puukko et al., 2018).

2.2. Experimental setup

Experimental setup resembled the in-situ TDE ongoing in Olkiluoto, Finland (Voutilainen et al., 2014). Tracer solution with known activities was injected to an injection hole and the diffusion and sorption of radionuclides from the injection hole water were analyzed. The breakthroughs of the tracer into four observation holes were monitored. The rock sample shown in Fig. 1 was veined gneiss with strong foliation

Fig. 1. The veined gneiss sample used in TDElab contained five experimental holes: A is the injection hole, B_1 and B_2 (the main direction of diffusion perpendicular to foliation) and C_1 and C_2 are the observation holes (the main direction of diffusion along foliation)). Dip of the foliation is 90°. The natural fracture inter connecting holes A, C1 and C2 can be seen in the upper part of the sample.

(seen vertically in the Fig. 1). The rock block was 30 cm in height and 30 cm in diameter. The injection hole (marked as A in the Fig. 1) was drilled in the middle of the rock and four observation holes were drilled around it. Observation holes B_1 and C_1 were 1 cm away from the injection hole and B_2 and C_2 were 4 cm away from the injection hole. Two of the observation holes (B_1 and B_2) were located so that the main direction of diffusion was perpendicular to the foliation and two other (C_1 and C_2) so that it was along the foliation.

The rock sample was saturated with synthetic REPRO groundwater (see Table 1) for five months before starting the experiment. Saturation was done by placing the rock sample in an experimental chamber that was filled with synthetic REPRO groundwater so that the upmost 1.8 cm of the rock sample was still over the water table. In addition, all five holes in the rock sample were filled with synthetic REPRO groundwater. The injection hole had a water volume of 63 mL whereas water volumes of the observation holes ranged from 13 to 14.5 mL. All holes were sealed with rubber caps to avoid evaporation. During the saturation synthetic REPRO groundwater was added to the holes twice a week to replace a decrease of water level. After saturation time of two months, the upper surface of the sample was completely moist due to capillary fringe and the rock sample was covered with epoxy resin in three stages. First, the bottom of the sample was sealed. This was followed by sealing of the lateral surface and the upper surface. The sealing was performed to ensure the complete saturation of the rock sample and to prevent the transport of radionuclides through the surface of the sample during the experiment. Saturation was continued after the epoxy treatment for two month by filling the experimental chamber half way with synthetic REPRO groundwater and the injection hole and four observation holes were also filled with synthetic REPRO groundwater. During this phase, the air was let to escape from the upper surface of the sample. One month before the injection the upper surface of the sample was sealed. During the last phase of saturation, it was made sure that the water level did not change in the experimental holes in order to ensure stationary conditions.

During the saturation of the sample, it was observed that the holes A, C_1 and C_2 were interconnected by a fracture that can be seen in the upper part of Fig. 1. The fracture was also observed in the drill cores samples. The examination of the drill core revealed that the fracture was of natural origin and that it had calcite filling.

The fracture groundwater in the Olkiluoto site is mainly of Na—Cl type with pH of 7.3–8.0. The groundwater is brackish at the depths from 40 m to 500 m. Concentrations of 9.0×10^{-4} to 1.1 mg/L of stable natural cesium and 8.1×10^{-2} to 2.6 mg/L of stable natural barium has been measured from Olkiluoto groundwater in previous studies (Hellä et al., 2014). Synthetic REPRO groundwater (pH 7.6) resembling the Olkiluoto groundwater in REPRO site was prepared for this experiment (see Table 1). It was decided to use simple simulant to represent the Olkiluoto groundwater because the chemical composition of this simulant is similar to the ONK-PP319 groundwater for the major elements which are chlorine, sodium and calcium. Other elements have concentrations so small that they do not have a significant effect on the salinity of the water. For this experiment, the synthetic REPRO groundwater contains all the elements from the Olkiluoto groundwater that are of importance for the diffusion and sorption studies of HTO, ^{36}Cl, ^{133}Ba and ^{134}Cs.

At the beginning of the experiment, the solution in the injection hole was replaced by 63 mL of tracer solution. Radioactive nuclides used in this experiment were HTO, ^{36}Cl, ^{133}Ba and ^{134}Cs. The ratios of the radionuclide activities was chosen to resemble the ratios used in the in-situ TDE. Table 2 shows the initial activities and concentration of HTO, ^{36}Cl, ^{133}Ba and ^{134}Cs used in TDElab. The concentrations of the radionuclides are relatively low and do not affect the concentrations given in Table 1. In in-situ TDE ^{22}Na was also used but in TDElab it was left out due to its high radiotoxicity in laboratory conditions. Usually in this type of experiments, ^{22}Na is used for the online monitoring of the breakthrough which was not necessary in this experiment due to continuous sampling.

The sampling of the injection hole was started one hour after the injection. The injection hole was sampled more frequently for the first two weeks during which total of 12 samples were collected. After the first two weeks, the injection hole was sampled every two weeks. Injection hole water sample volume was 0.1 mL and the sample volume was replaced with pure synthetic REPRO groundwater in every sampling. The 0.1 mL injection hole water sample was diluted to 5 mL with synthetic REPRO groundwater to achieve a calibrated sample geometry of gamma measurement. The activities of the samples were decay corrected to the activity at moment of the injection according to the half-lives given in Table 2. Water level remained constant in all experimental holes during the experiment indicating that there advection did not affect the results and the transport of tracers was purely caused by diffusion.

Table 1
The chemical composition of synthetic REPRO groundwater that was constructed according to the main components of groundwater samples collected from the REPRO site (Poteri et al., 2018).

Anion/cation	Concentration (mg/L)
Ca^{2+}	520
Na^{+}	2810
Cl^{-}	5250

Table 2
The half-lives of HTO, ^{36}Cl, ^{133}Ba and ^{134}Cs and their initial activities and concentrations in the injection hole applied in TDElab.

Radionuclide	Initial activity, A_0 (kBq)	Half-life, $t_{1/2}$ (y)	Initial concentration, C_0 (mg/L)
H^3 (HTO)	173.8 ± 2.1	12.32	$(5.14 \pm 0.07) \times 10^{-5}$
^{36}Cl	99.8 ± 3.0	3.01×10^5	1.30 ± 0.04
^{133}Ba	77.5 ± 1.9	10.51	$(1.30 \pm 0.04) \times 10^{-4}$
^{134}Cs	27.3 ± 0.3	2.065	$(9.05 \pm 0.10) \times 10^{-6}$

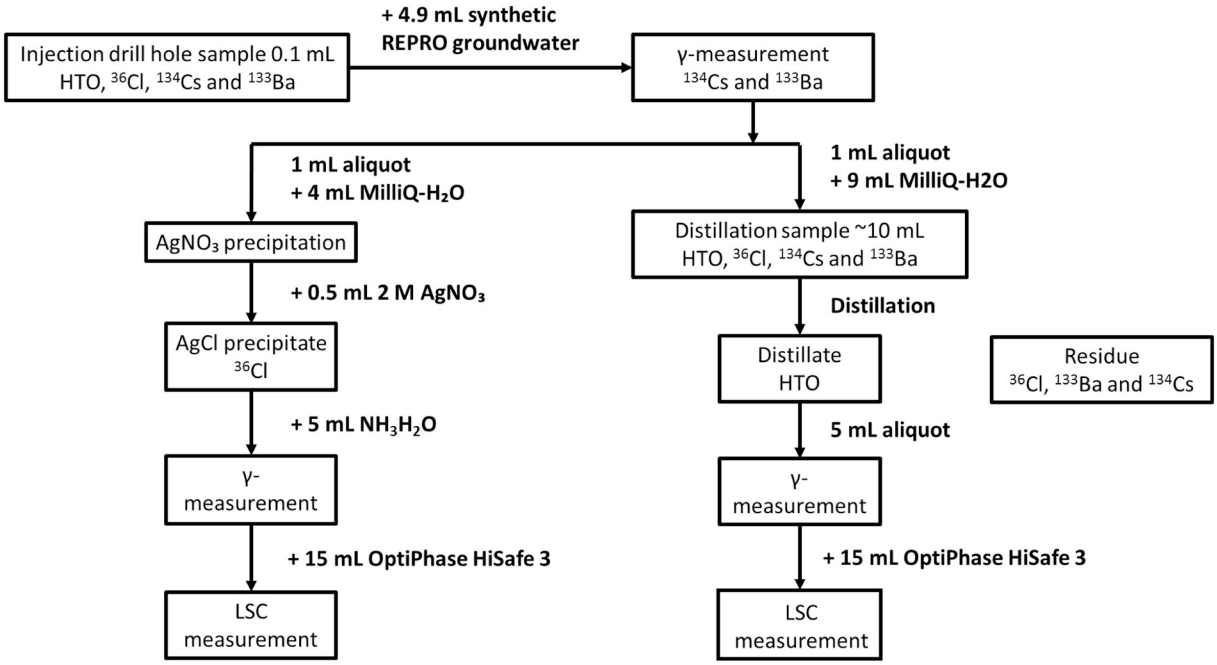

Fig. 2. An analysis method for determining activities of HTO, ^{36}Cl, ^{133}Ba and ^{134}Cs from groundwater samples.

2.3. Water analyses

^{3}H (radioactive nuclide in HTO) and ^{36}Cl are pure beta emitters and their activities were measured with liquid scintillation counting (LSC, Perkin Elmer Tri-Carb 2910 TR, spectrum analyzer SpectraWorks). However, gamma emitting radionuclides ^{133}Ba and ^{134}Cs also have beta or electron emissions that will interfere ^{3}H and ^{36}Cl measurements. Therefore, in order to measure beta emitting ^{3}H and ^{36}Cl from the groundwater solution the gamma emitting radionuclides need to be separated from them. The separation was done according to an analysis method developed for the in-situ TDE groundwater samples (Aromaa et al., 2018) shown in Fig. 2.

The activities of gamma emitting radionuclides ^{133}Ba and ^{134}Cs were measured with a HPGe-detector (Canberra XtRa; Extended Range Coaxial HPGe Detector with spectral analysis program Gamma Acquisition and Analysis Genie/Canberra). After gamma measurement, 1 mL subsample (A1) of the injection hole water sample was taken for the analysis of ^{36}Cl activity. The subsample was diluted to 5 mL by MilliQ-H_2O (deionized using Milli-Q, Millipore Co) and ^{36}Cl was separated from it by $AgNO_3$ precipitation. Precipitation was performed by adding 0.5 mL of 2 mol/L $AgNO_3$ solution to the A1 sample. The chlorine concentration of the synthetic REPRO groundwater (5000 mg/L) secures high enough chlorine content in the A1 sample so that no additional carrier is needed. The chlorine concentration in the A1 sample is 0.14 M and the $AgNO_3$ concentration is 0.2 M which is enough for the precipitation of all chlorine in the sample as AgCl. The precipitate was washed twice with 5 mL MilliQ-H_2O to ensure a clean sample for LSC. The AgCl precipitate was dissolved in 5 mL ammonia and measured with the HPGe-detector for any gamma emitting residue that might have been left in the sample bottle. The ^{36}Cl sample, clean from disturbing spectral components, was mixed with 15 mL of liquid scintillation cocktail (OptiPhase HiSafe 3, Perkin Elmer) and measured with LSC. Yields of 98 ± 2% for AgCl precipitation was determined in the previous work for similar water samples (Aromaa et al., 2018).

For the separation of HTO, another 1 mL subsample (A2) of the injection hole water sample was diluted to 10 mL with MilliQ-H_2O. HTO was separated from the A2 subsample by distillation. The 10 mL sample was heated with a thermophore and the vapor was condensed in a water circulation condenser. Distillate that contained tritium as tritiated water (HTO) was collected into a round bottomed flask. 5 mL aliquot of the distillate was measured with the HPGe-detector for any gamma emitting residue. The clean residue was mixed with 15 mL liquid scintillation cocktail and measured with LSC for ^{3}H activity. The 10 mL distillation sample as well as the distillate were weighed for recovery determination. In the previous work, the recoveries of 74 ± 6% for distillation were achieved for similar water samples (Aromaa et al., 2018).

Observation holes were sampled once a week. A 5 mL subsample of the water was used for the analysis of gamma emitting radionuclides ^{133}Ba and ^{134}Cs by using the HPGe-detector. In case of no gamma emitting radionuclides in the observation hole water sample, the subsample was mixed with 15 mL of liquid scintillation cocktail and the activities of ^{3}H and ^{36}Cl were measured directly with LSC using separation of ^{3}H and ^{36}Cl by their β-energies. In case of a disturbing beta/electron emitters in the water sample, the separation of HTO and ^{36}Cl was in the same way as the injection hole water samples.

2.4. Time-domain random walk simulations

It is not possible to analyze the results of the diffusion experiments using analytical tools due to complicated geometries of the experimental systems and sampling procedure of the injection and observation holes. We modeled the transport of tracer nuclides using the TDRW method as this approach can handle heterogeneous geometries and concentrations. The approach is also generally convenient with large systems since computation times do not considerably depend on sample size, and it is faster than more traditional simulation methods (Sardini et al., 2003). A more detailed description of the theory is given by Delay et al. (2002), Sardini et al. (2003), and Voutilainen et al. (2017) so only a brief outline is given here.

A diffusing unit of mass is defined as a particle which is forced to jump during a transition time to one of its neighboring voxel on a mesh defining the diffusion space. The transition probability (P_{ij}) of a particle in a voxel i to a neighboring voxel j is defined by:

$$P_{ij} = \frac{b_{ij}}{\sum_j b_{ij}} \quad (1)$$

where

$$b_{ij} = \frac{A_{ij}(D_e)_{ij}}{L_{ij}} \quad (2)$$

with A_{ij} the total area between the voxels i and j, $(D_e)_{ij}$ the harmonic mean of the effective diffusion coefficient (D_e) at voxels i and j, and L_{ij} the distance between the centers of the voxels i and j. The transition probability of a jump by a particle at a site i is taken into account such that, reaching the target site takes certain time, the transition time, which depends on the properties of the two voxels. The transition time for a jump from the voxel i to the voxel j is given by

$$t_{i\to j} = -\frac{\varepsilon_i V_i}{\sum_j b_{ij}} \log(u_{01}) \quad (3)$$

where V_i is the total volume of the voxel i and u_{01} a random number from a uniform distribution between 0 and 1. The Eq. (3) defines the transition time due to diffusion from the voxel i to the voxel j but it does not take into account possible sorption of the particles. Recently, Voutilainen et al. (2017) developed the TDRW method further so that it is possible to account for the sorption of particles using K_d-concept. The distribution coefficients (K_d) are typically measured for geological samples and they define the chemical strength of sorption. Voutilainen et al. (2017) proposed expression for sorption time (t_s) during the transition:

$$t_s = -\frac{\varepsilon_i V_i}{\sum_j w_{ij}} \log(u_{01}) - \left(-\frac{\varepsilon_i V_i}{\sum_j b_{ij}} \log(u_{01})\right) \quad (4)$$

where

$$w_{ij} = \frac{A_{ij}(\varepsilon D_a)_{ij}}{L_{ij}} \quad (5)$$

with $(\varepsilon D_a)_{ij}$ the harmonic mean of the product of porosity and apparent diffusion coefficient (D_a) at the voxels i and j. In D_a the effect of sorption is taken into account

$$D_a = \frac{D_e}{\varepsilon + (1-\varepsilon)\rho K_d} \quad (6)$$

where ρ is the density of rock.

A 3D 8-bit greyscale image was constructed for the simulations using ImageJ. The 3D image was used as the simulation geometry where voxels formed a simulation mesh. The grayscale image has 256 possible grayscale values for each voxel. The mesh was created according to the actual dimensions of the rock sample so that one voxel represents $(1 \times 1 \times 1)$ mm^3 sized cube. This led to a cylindrical simulation mesh with the size of $290 \times 290 \times 280$ (see Fig. 3a). In the 3D image, each component (rock, fracture, injection hole and observation holes) were colored with a unique grey-scale value (see Fig. 3b) which was linked to its porosity, diffusion coefficient and distribution coefficient. Unique grey values were also used to assist the sampling during the simulation by checking the grey value of the voxel where the particle is located after experimental sampling time has been reached (see steps 3 and 4 in simulation procedure below).

Due to the observed fracture, interconnecting holes A, C_1 and C_2 (see Sec. 2.2), a simple planar fracture with individual properties was added into the simulation mesh (see Fig. 3). The real fracture is of course more heterogeneous and it is simplified in our conceptual model. The effective diffusion (D_e) and porosity of the intact rock and the fracture applying HTO and ^{36}Cl data were first modeled using the measured concentration of injection hole as source. This was followed by determination of the distribution coefficients of intact rock and fracture coatings for ^{133}Ba and ^{134}Cs by assuming the same D_e and porosity as for HTO. Here the distribution coefficient of the intact rock and fracture coating were varied in order to find agreement between measured and modeled breakthrough curves.

The simulations were done using 5×10^5 particles for the non-sorbing nuclides and 1×10^6 for the sorbing nuclides. The initial position for each particle was chosen randomly in the injection hole. The porosity, diffusion coefficient and distribution coefficient in the injection and observation holes were set to 100%, D_0 in free water, and no sorption applied, respectively. During the simulation following procedure was repeated until a preset total diffusion time was elapsed:

1. Determine the direction of a jump according to the transition probabilities (see Eq. (1)) and a selected random number.
2. Determine transition and sorption times according to Eqs. (3) and (4), and a second random number.
3. Check if experimental sampling time has passed during the jump. If not, return to point 1.
4. Check if the particle is in one of the holes. If not, return to point 1.
5. Record the location of particle and remove part of the particles according to a third random number. The ratio of removed particles is set according to the sample volume and total volume of the hole in which the particle is currently located.
6. Check if total diffusion time is elapsed. If not, return to point 1.

The fitting of simulated curves to experimental curves was performed by determining the sum of squared deviation for each parameter pair and by finding a minimum of the sum (least squared approach). The confidence limits for simulated curves were defined so that the measured curves remained within the limits and that concentration changes in the injection and observation holes could be explained using similar values for the porosity, effective diffusion coefficient and distribution coefficient (in case of sorbing nuclides).

3. Results

3.1. Injection hole

Total of 34 samples were collected from injection hole A during 39 weeks experimental time. The activities of gamma emitting ^{133}Ba and ^{134}Cs were measured with the HPGe-detector. Activities of HTO and ^{36}Cl were determined by separating the radionuclides from ^{133}Ba and ^{134}Cs. Separated HTO and ^{36}Cl were measured with LSC without spectral interferences. Fig. 4 shows the decrease of the relative concentrations of four radionuclides in the injection hole as a function of time.

In Fig. 4, the concentrations of ^{133}Ba and ^{134}Cs decreased rapidly at the beginning of the experiment. Especially the concentration of ^{134}Cs decreased to almost tenth of its original value during the first month of the experiment. The decrease of ^{133}Ba was more modest and the concentration decreased to sixth of the original value during the first month of the experiment. The rapid decrease in the activities of ^{133}Ba and ^{134}Cs can be explained by their strong sorption onto mineral surfaces that are in direct contact with tracer solution. The rapid drop is followed by a steady decrease of concentration due to in-diffusion into rock and sorption on minerals surfaces within the transport routes. The difference between the relative concentrations of ^{133}Ba and ^{134}Cs can be explained by a difference in their distribution coefficients.

The concentrations of HTO and ^{36}Cl decrease modestly during the whole experiment. The steady decrease is caused by in-diffusion into the rock and relatively small effective diffusion coefficient. A slight difference in the decrease rate between HTO and ^{36}Cl can be explained by the difference in the diffusion coefficients in water what is slightly lower for ^{36}Cl (D_0(HTO) = 2.22×10^{-9} m^2/s (Jones et al., 1965) and D_0(Cl-36) = 2.06×10^{-9} m^2/s (Hawlicka, 1987)). After 39 weeks of the experiment, only 4.9% of ^{134}Cs (4.9% if sample collection is taken into account) and 17.6% of ^{133}Ba (17.9%) was left in the injection hole. From the non-sorbing HTO and ^{36}Cl radionuclides 54% (56%) and 63% (66%), respectively, was left in the injection hole in the end of the experiment.

During the saturation, it was observed that the holes A, C_1 and C_2 were interconnected by a fracture. Furthermore, it is known that veined

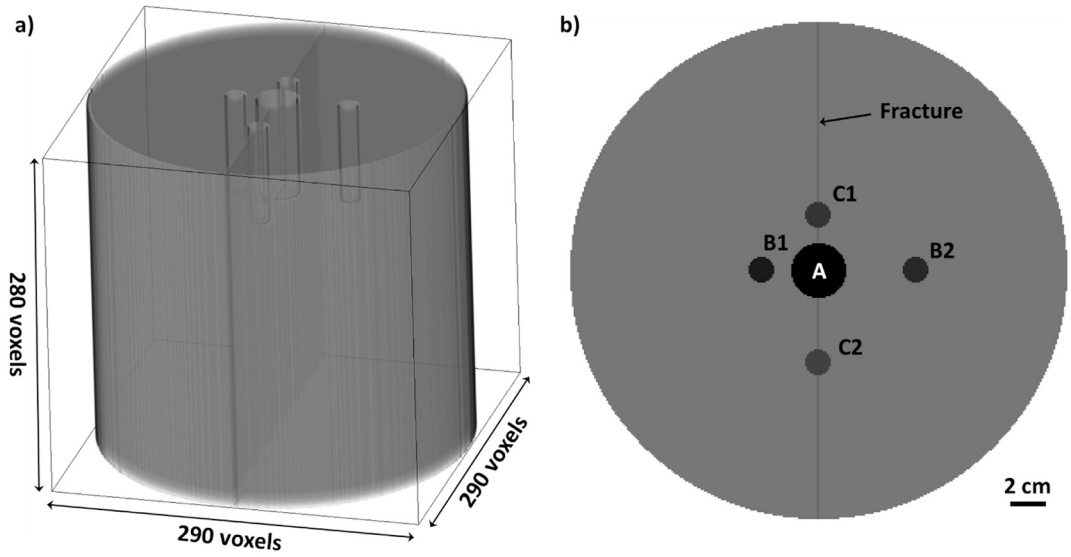

Fig. 3. a) The three dimensional presentation of the 290 × 290 × 280 voxel sized simulation mesh that was used in the modeling. The size of one voxel was 1 mm^3. b) A 2D cross section of the mesh showing the rock matrix (grey value: 100) and the location of the injection hole A (0), fracture (80) and observation holes B1 (20), B2 (30), C1 (40) and C2 (50).

gneiss samples from Olkiluoto have structure with banded foliation and that transport of elements may be different across and along the foliation (Kärki and Paulamäki, 2006). Due to the presence of the fracture, possible effect of foliation and heterogeneity of VGN (Voutilainen et al., 2019), it was not possible to model data from both injection and observation holes simultaneously. Hence, the measured concentrations in the injection hole were used as the source term in the TDRW modeling (see solid lines in Fig. 4). In the simulations, the correct boundary condition was kept by adding particles to or removing them from the injection hole (if needed) at each measurement point (see Fig. 4).

3.2. Diffusion of non-sorbing nuclides

Observation holes were sampled once a week starting from one week from the injection. Total of 39 samples were collected per observation hole during 39 weeks experimental time. The breakthrough curves were modeled by TDRW method using the measured concentration in injection hole A as a source. Fig. 5 shows the measured and modeled breakthrough curves for HTO and ^{36}Cl to observation holes B_1, B_2, C_1 and C_2. Breakthrough of HTO and ^{36}Cl was observed in all four observation holes and the breakthrough curves were successfully modeled using TDRW simulations.

The breakthrough curves of HTO and ^{36}Cl are similar for all of the observation holes (see Fig. 5) and the transport of these non-sorbing nuclides does not depend on radionuclide in question. The breakthrough of HTO tends to be slightly faster than of ^{36}Cl. This can be explained by small difference in the diffusion coefficients in water. The values for the effective diffusion coefficient and porosity determined from the observation holes B_1 and B_2 represent the properties of intact rock (see Table 3). There is a small difference in the effective diffusion

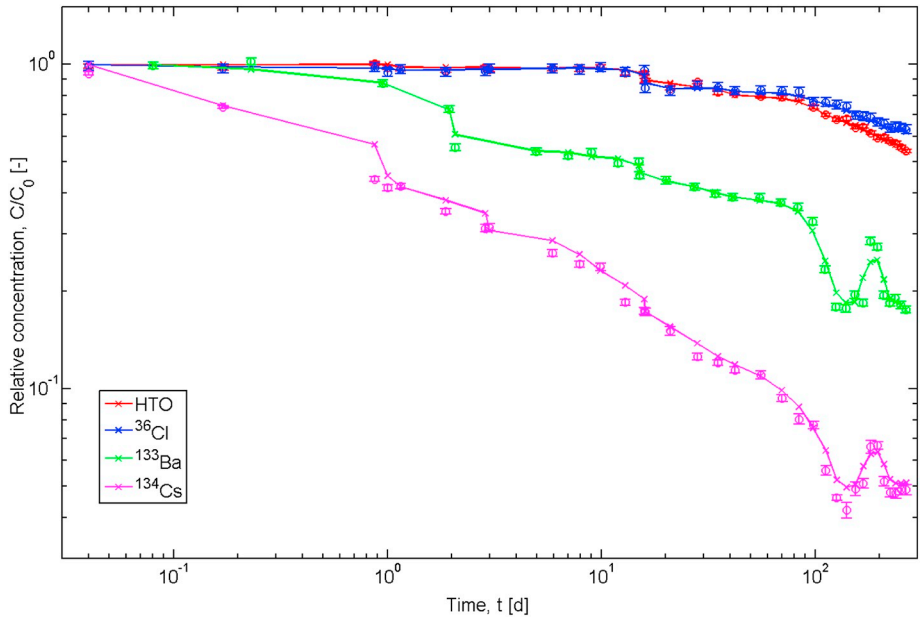

Fig. 4. Relative concentration (C/C_0) of HTO, ^{36}Cl, ^{133}Ba and ^{134}Cs, in the injection hole A as a function of time. The solid lines show the concentration set for the modeling.

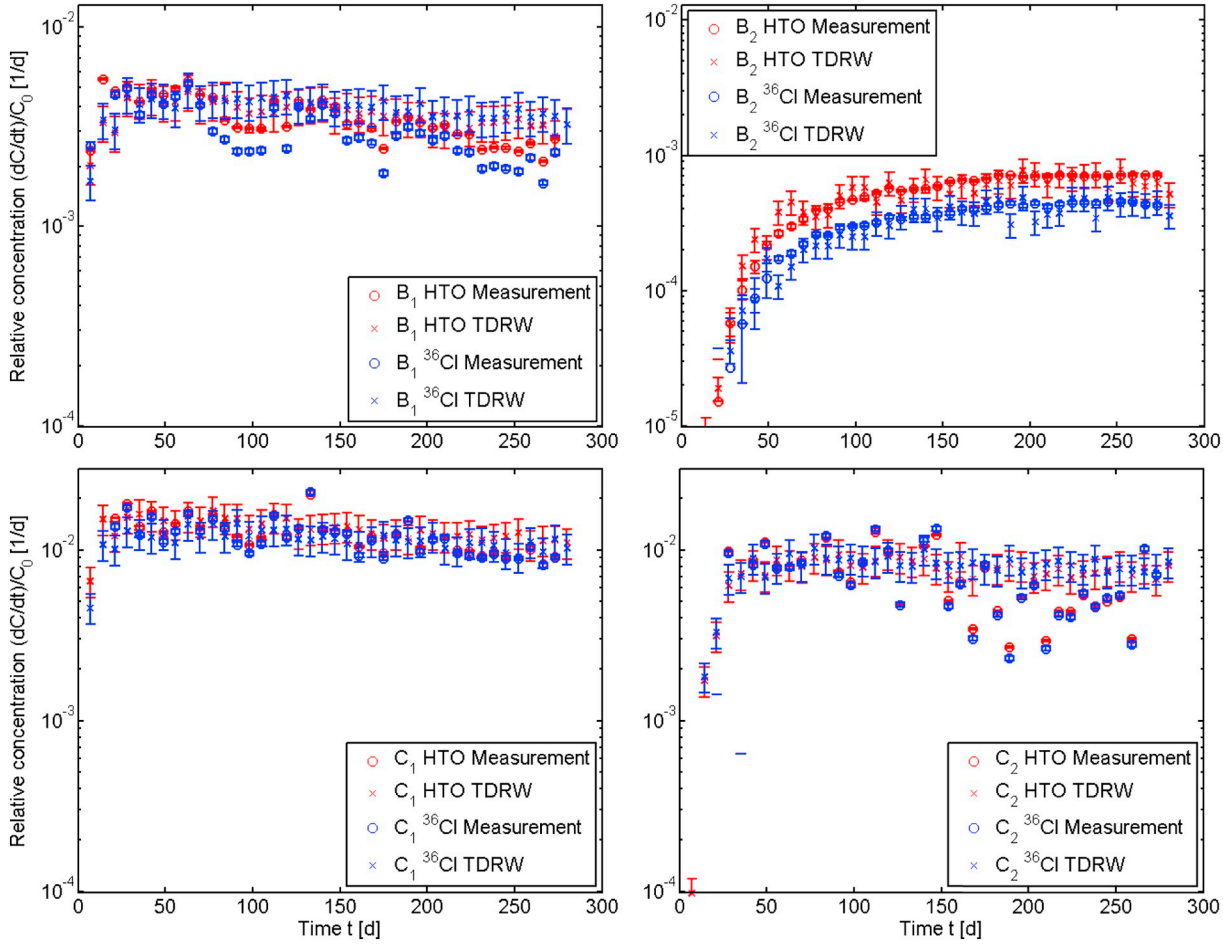

Fig. 5. Measured (circles) and modeled (crosses) breakthrough curves for HTO (red) and ^{36}Cl (blue) to observation holes B_1 and B_2 (Upper panels, foliation perpendicular to the main diffusion direction) and C_1 and C_2 (Lower panels, foliation along the main diffusion direction) as a function of time. Error bars show the uncertainties of experimental and modeled data. Note that the scaling of y-axis varies. (For interpretation of the references to colour in this figure legend, the reader is referred to the web version of this article.)

coefficients of HTO and ^{36}Cl determined from observation holes B_1 and B_2. The difference is caused by the difference in diffusion coefficients in free water. Furthermore, the uncertainties of the effective diffusion coefficients overlap. The effective diffusion coefficients determined from the breakthrough curves of B_1 are about a factor of two larger than of B_2. The porosities determined from these breakthrough curves are in agreement.

The values determined from the breakthrough curves of HTO and ^{36}Cl to the observation holes C_1 and C_2 represent mostly the properties of the fracture and are about two orders of magnitude higher than those of the intact rock (see Table 3). Clearly, the observed fracture increases the transport in the direction of foliation and thus the effect of foliation on diffusion cannot be seen from the results. However, the measured curves could not be modeled using a porosity of 100% and diffusion coefficient of free water. This indicates that the simplified planar fracture cannot fully explain the properties of the natural and heterogeneous fracture that has a varying aperture. Furthermore, the effect of fracture heterogeneity is seen in the difference of effective diffusion coefficients determined for C_1 and C_2.

3.3. Diffusion and sorption of sorbing nuclides

The measured and modeled breakthrough curves of ^{133}Ba and ^{134}Cs to observation holes B_1, C_1 and C_2 are shown in Fig. 6. No breakthrough of sorbing nuclides was observed in observation hole B_2 and ^{134}Cs was observed only in the C_1 that was closest to the injection hole and along the fracture. All of the measured breakthrough curves were successfully modeled using TDRW simulations.

The breakthrough of sorbing nuclides is restrained in comparison with the breakthrough of the non-sorbing nuclides. However, the

Table 3
Effective diffusion coefficients, porosities and distribution coefficients determined from the breakthrough curves of HTO, ^{36}Cl, ^{133}Ba and ^{134}Cs to the observation holes (B_1, B_2, C_1 and C_2).

	HTO		^{36}Cl		^{133}Ba		^{134}Cs	
	$D_e \times 10^{-13}$ [m^2/s]	Porosity [%]	$D_e \times 10^{-13}$ [m^2/s]	Porosity [%]	$D_e \times 10^{-13}$ [m^2/s]	$K_d \times 10^{-4}$ [m^3/kg]	$D_e \times 10^{-13}$ [m^2/s]	$K_d \times 10^{-4}$ [m^3/kg]
B_1	8.0 ± 1.0	0.7 ± 0.1	7.0 ± 1.0	0.7 ± 0.1	4.4 ± 1.0	1.0 ± 0.3	–	–
B_2	3.5 ± 1.0	0.8 ± 0.1	3.0 ± 1.0	0.8 ± 0.1	–	–	–	–
C_1	400 ± 100	90 ± 5	400 ± 100	90 ± 5	220 ± 50	1.0 ± 0.3	380 ± 100	20 ± 5
C_2	800 ± 100	90 ± 5	800 ± 100	90 ± 5	440 ± 100	1.0 ± 0.3	–	–

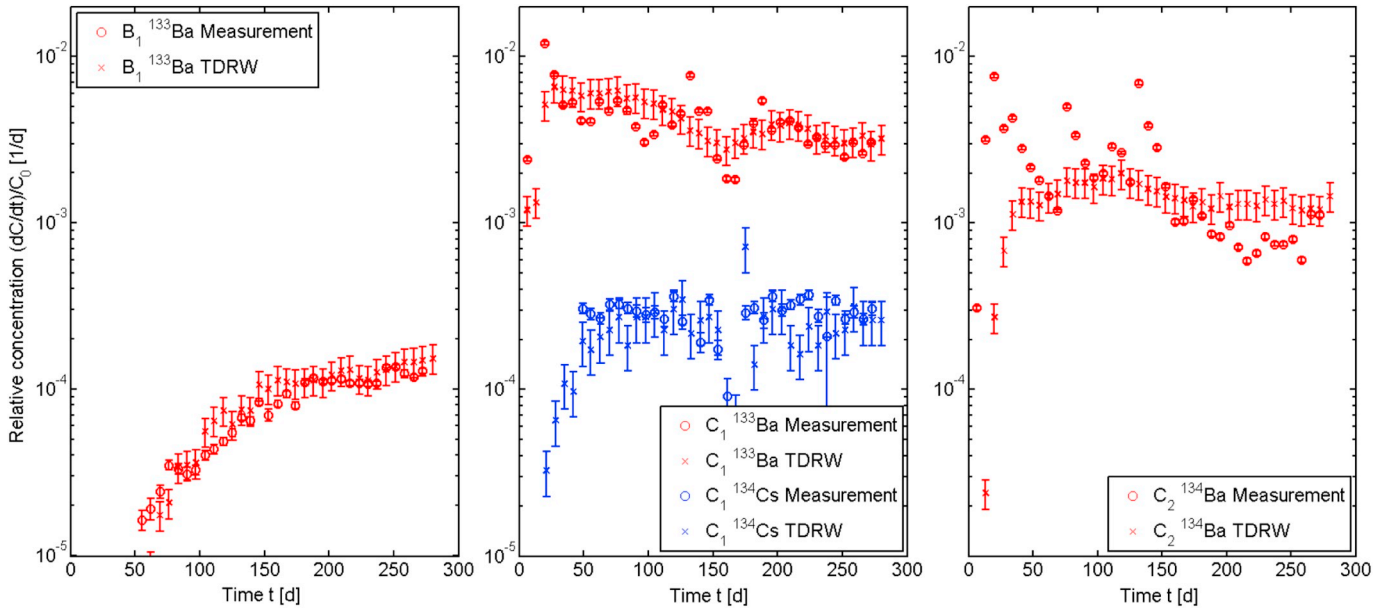

Fig. 6. Measured and modeled breakthrough curves for ^{133}Ba and ^{134}Cs to observation holes B_1 (Left panel, foliation perpendicular to the main diffusion direction), and to C_1 (middle panel) and C_2 (Right panel) (foliation along the main diffusion direction) as a function of time. Error bars show the uncertainties of experimental and modeled data.

shapes of the breakthrough curves are similar. In the TDRW modeling, the effective diffusion coefficients were adjusted according to the ones determined for HTO by scaling it using the diffusion coefficients of ^{133}Ba and ^{134}Cs in free water ($D_0(^{133}Ba) = 1.22 \times 10^{-9}$ m^2/s (Vitagliano and Lyons, 1956) and $D_0(^{134}Cs) = 2.09 \times 10^{-9}$ m^2/s (Friedman and Kennedy, 1955)) and porosities from HTO measurements were used. Then the distribution coefficients were adjusted so that agreement between measured and modeled data was found. All three measured breakthrough curves of ^{133}Ba could be explained using the distribution coefficient of $(1.0 \pm 0.3) \times 10^{-4}$ m^3/kg. According to these results it can be concluded that the minerals adjacent to the fracture have similar sorption properties than the main rock and alteration has not changed considerably the sorption capacity of the rock compared with the intact rock. The distribution coefficient of ^{134}Cs for minerals adjacent to the fracture determined from the breakthrough curve of observation hole C_1 was $(20 \pm 5) \times 10^{-4}$ m^3/kg.

4. Discussion and summary

HTO and ^{36}Cl reached all of the observation holes while a significant breakthrough of ^{134}Cs was found only in the hole C_1 and ^{133}Ba in the holes B_1, C_1 and C_2. Furthermore, it was observed that the rock core contained a fracture that crosses the holes A, C_1 and C_2 and creates a fast transport route between these holes. Thus, the transport parameters determined by the modeling are very different for B and C holes (see Table 3). The values given to observation holes B_1 and B_2 represent the properties of the intact rock while the values given to observation holes C_1 and C_2 are influenced by the fracture that was found to interconnect observation holes C_1 and C_2 with injection hole A. Due to the effect of the fracture it was not possible to model reliably the decrease of concentration in injection hole A simultaneously with the breakthrough curves to observation holes B_1, B_2, C_1 and C_2 and thus the concentration in the injection hole was used as the source concentration in the TDRW modeling (see Section 3.1). In general, TDElab serves as good demonstration how the heterogeneity of the rock may interfere in the through diffusion measurements and how difficult it can be to determine the properties of the rock using a single hole experiments.

The porosities determined for the VGN sample are in agreement with the previous results for samples from REPRO site and other location in Olkiluoto (Ikonen et al., 2015; Kuva et al., 2015; Sammaljärvi et al., 2017; Smellie et al., 2014). In these studies, average porosities of (0.8 ± 0.5) % (Ikonen et al., 2015) and (0.7 ± 0.3) % (Smellie et al., 2014) has been reported for VGN samples from the REPRO site and unaltered VGN samples from Olkiluoto, respectively. Hence it can be concluded that the porosity of VGN sample represents the typical values in the REPRO site and in Olkiluoto in general.

Smellie et al. (2014) report effective diffusion coefficients of $(1.0 \pm 0.4) \times 10^{-13}$ m^2/s and $(0.2 \pm 0.2) \times 10^{-13}$ m^2/s for HTO and ^{36}Cl, respectively, in unaltered VGN samples from Olkiluoto while Voutilainen et al. (2018) report slightly higher values for HTO (1.0×10^{-13}–4.8×10^{-13} m^2/s) and ^{36}Cl (0.05×10^{-13}–3.4×10^{-13} m^2/s) in VGN samples from the REPRO site. The effective diffusion coefficients determined from the breakthrough curve to B_1, which is one centimeter away from the injection hole, are slightly larger than the previously determined values and they are possibly affected by the drilling induced opening of the micrometer scale pores and grain boundaries when preparing the injection and observation holes. Furthermore, in short distances (~2–3 times grain size) the connectivity of the pore space is typically better than at longer distances (~10 times grain size) (Glover and Walker, 2009). For example, Hartikainen et al. (1996) have shown that sample preparation affect the effective diffusion coefficient in short length scales. However, the effective diffusion coefficients determined from the breakthrough curve to B_2 are reasonable and they are within the upper limit of the previous results for samples from REPRO site. Based on these considerations it can be concluded that the diffusion coefficients of HTO and ^{36}Cl in the intact VGN sample are of $(3.5 \pm 1.0) \times 10^{-13}$ m^2/s and $(3.0 \pm 1.0) \times 10^{-13}$ m^2/s, respectively.

In some previous experiments performed for samples from Olkiluoto, an effect of anion exclusion has been detected (e.g. Smellie et al., 2014; Voutilainen et al., 2016, 2018). This has been seen as a smaller effective diffusion coefficient of ^{36}Cl than of HTO and is caused by electrical repulsion between negatively charged mineral surfaces and chloride ions. The anion exclusion was not, however, observed in TDElab and the difference between the effective diffusion coefficients of ^{36}Cl and HTO can be explained by the difference of their diffusion coefficients in free water. Lately, it has been argued that the alteration state of the minerals within the transport pathways may have

considerable effect on the presence of anion exclusion (Sammaljärvi et al., 2017). The VGN sample was found to be fractured that has plausibly increased the pore apertures and thus decreased effect caused by anion exclusion.

It was shown that the breakthrough curves of sorbing radionuclides could be modeled by adjusting only the distribution coefficient and using the porosities and scaled effective diffusion coefficients determined from the breakthrough curves of HTO. This approach resulted in a perfect agreement between the measured and modeled breakthrough curves and thus completely independent fitting was not needed. This demonstrates that HTO and sorbing nuclides are diffusing similarly in the system (if sorption is neglected) and build confidence on the applied model.

Previously, Muuri et al. (2018) have reported the distribution coefficients of 0.1 m^3/kg and 1.1×10^{-3} m^3/kg for ^{133}Ba determined in batch sorption experiments for crushed VGN and 1 cm^3 cube of VGN, respectively, from REPRO site. The distribution coefficient of ^{133}Ba determined for TDElab sample is about three orders of magnitude smaller than the value for the crushed rock and one order of magnitude smaller than the value for the rock cube. It is obvious that the distribution coefficients determined for crushed material overestimates the distribution coefficient of intact rock due to increased specific surface area caused by the crushing. Muuri et al. (2018) reached the same conclusion. However, the difference between the results for the rock cube and TDElab is not that straight forward. The main difference of the measurements is the experimental design. In study performed by Muuri et al. (2018), the distribution coefficients are determined from the concentration decrease in surrounding tracer solution (in-diffusion experiment) while in TDElab they are determined using the breakthrough curves. In the in-diffusion experiment, the early part of the in-diffusion curve is dominated by the sorption of the tracer on fresh mineral surfaces on the surface of the sample. This is seen as a rapid drop in the concentration (Muuri et al., 2018). This effect can also be seen in the Fig. 4. Note that such situation also describes the case where radionuclides are being transported by fracture flow and are in contact with minerals on fracture surfaces. In the through-diffusion experiment, the mineral surfaces inside the rock sample have greater influence on the breakthrough curve than the mineral surfaces on drill hole wall and thus the distribution coefficients determined this way better represent the distribution coefficients of intact rock. Note here that the distribution coefficients of ^{133}Ba determined for all measured breakthrough curves gave the same results. Based on this it can be concluded that the observed fracture has not affected the sorption properties of the rock in comparison with the rest of the rock.

If we assume that the same conclusion made above for ^{133}Ba applies also for ^{134}Cs, the distribution coefficient $(20 \pm 5) \times 10^{-4}$ m^3/kg can be considered as the distribution coefficient of ^{134}Cs for intact rock. Recent study by Muuri et al. (2017), show the distribution coefficients of 0.092 m^3/kg and 0.031 m^3/kg for ^{134}Cs determined in batch sorption experiments for crushed VGN and 1 cm^3 cube of VGN, respectively, from REPRO site. The distribution coefficient of ^{134}Cs determined for TDElab sample is about two orders of magnitude smaller than the value for the crushed rock and one order of magnitude smaller than the value for the rock cube. The conclusions made for ^{133}Ba regarding the increase of specific surface area and effect of experimental design seem to be valid also for ^{134}Cs and thus these observations strengthen the conclusions. The fact that cesium reached only one of the observation holes is due to the relatively high sorption. In fact with given parameters and used total number of particles, it was not possible to get any particles into the other observations holes. This is consistent with the measurements.

Unfortunately, it was not possible to model the data from all of the experimental holes simultaneously and thus the measured concentrations in the injection hole were used as the source term when modeling breakthrough to observation holes. However, the source term remains as identical with the measured concentration (see Fig. 4). When considering the transport of tracers from the injection hole to one of the observation holes, the dominant behavior comes from the direction that has the shortest distance. Due to this, we are able to catch the dominant behavior even though the other directions are not modeled precisely right at the same time. This was demonstrated by showing that the simulations were able to reproduce the breakthrough curves similar to the measured ones. This would not be the case if the dominant behavior would not be modeled correctly. Note that the dominant behavior is the most important from the perspective of safety assessment. When considering the simplifications made in the conceptual model (see Fig. 3), the performance of the model can be considered relatively good.

The properties of the fracture are obviously heavily simplified by the conceptual model. Looking beyond the aims and results this study, the conceptual model could be improved by (i) characterizing the structure and properties of the fracture, (ii) characterizing the mineral structure of the sample and (iii) adding effect caused by the foliation of the rock. These characterizations could be performed using e.g. microcomputed tomography and C-14-PMMA autoradiography (Voutilainen et al., 2017). Furthermore, the characterization study could be combined with a detailed study of sorption of barium and cesium on different minerals of the rock. This study would reveal how the sorbing nuclides have been transported in the intact rock and vicinity of the calcite filled fracture. The latter study would also assist the sample analyses of the in-situ experiment after the over-coring.

5. Conclusions

The through diffusion experiment in the laboratory was introduced. TDElab was performed using HTO, ^{36}Cl, ^{133}Ba and ^{134}Cs as tracers and modeled using TDRW modeling. The effective diffusion coefficients and distribution coefficients of radionuclides and the porosity of the rock were determined applying the through diffusion type of experiments in the decimeter scale rock sample. These parameters are of great importance when assessing the ability of bedrock to retard the transport of radionuclides towards biosphere. The porosity and effective diffusion coefficients of HTO and ^{36}Cl were found to be in agreement with previously determined values for REPRO samples. The distribution coefficients of ^{133}Ba and ^{134}Cs were two to three orders of magnitude lower than those obtained previously for crushed Olkiluoto rock. Furthermore, the distribution coefficients were one order of magnitude lower than those obtained from the in-diffusion experiments. It was concluded that the differences are caused by increased specific surface area and sorption capacity due to crushing in the first case and different experimental design in the latter case.

In the future, the determined porosities, effective diffusion coefficients and distribution coefficients can be compared with ones from in-situ TDE that has similar experimental design. The comparison will give information about the effect of experimental conditions on the rock properties. In case there will be considerable difference in the results, the comparison enables the conversion of the previous results from laboratory experiments into conditions analogous to those at the repository site. Furthermore, the produced site specific data can be readily used in the safety assessment of the repository as conservative estimates.

Acknowledgements

The financial support by Posiva Oy is gratefully acknowledged.

References

Aalto, P., Aaltonen, I., Ahokas, H., Andersson, J., Hakala, M., Hellä, P., Hudson, J., Johansson, E., Kemppainen, K., Koskinen, L., Laaksoharju, M., Lahti, M., Lindgren, S., Mustonen, A., Pedersen, K., Pitkänen, P., Poteri, A., Snellman, M., Ylä-Mella, M., 2009. Programme for Repository Host Rock Characterisation in the ONKALO (ReRoC) (Posiva Working Report 2009-31, Posiva Oy, Eurajoki, Finland). https://doi.org/10.1007/s00259-009-1174-1.

Aaltonen, I., Engström, J., Gehör, S., Kosunen, P., Kärki, A., Mattila, J., Paananen, M., Paulamäki, S., 2016. Geology of Olkiluoto. (Posiva Report 2016-16, Posiva Oy, Eurajoki, Finland).

Andersson, P., Byegård, J., Tullborg, E.-L., Doe, T., Hermanson, J., Winberg, A., 2004. In situ tracer tests to determine retention properties of a block scale fracture network in granitic rock at the Äspö Hard Rock Laboratory, Sweden. J. Contam. Hydrol. 70, 271–297. https://doi.org/10.1016/j.jconhyd.2003.09.009.

André, M., Malmström, M.E., Neretnieks, I., 2009. Determination of sorption properties of intact rock samples: new methods based on electromigration. J. Contam. Hydrol. 103, 71–81. https://doi.org/10.1016/j.jconhyd.2008.09.006.

Aromaa, H., Helariutta, K., Ikonen, J., Yli-Kaila, M., Koskinen, L., Siitari-Kauppi, M., 2018. Analysis of ^{3}H, ^{36}Cl, ^{22}Na, ^{133}Ba and ^{134}Cs from synthetic granitic groundwater: an in situ through diffusion experiment at ONKALO. J. Radioanal. Nucl. Chem. 318, 1161–1169. https://doi.org/10.1007/s10967-018-6139-z.

Delay, F., Porel, G., Sardini, P., 2002. Modelling diffusion in a heterogeneous rock matrix with a time-domain Lagrangian method and an inversion procedure. Compt. Rendus Geosci. 334 (13), 967–973. https://doi.org/10.1016/S1631-0713(02)01835-7.

Dentz, M., Gouze, P., Russian, A., Dweik, J., Delay, F., 2012. Diffusion and trapping in heterogeneous media: an inhomogeneous continuous time random walk approach. Adv. Water Resour. 49, 13–22. https://doi.org/10.1016/j.advwatres.2012.07.015.

Friedman, A.M., Kennedy, J.W., 1955. The self-diffusion coefficients of potassium, cesium, iodide and chloride ions in aqueous solutions. J. Am. Chem. Soc. 77, 4499–4501. https://doi.org/10.1021/ja01622a016.

Gjetvaj, F., Russian, A., Gouze, P., Dentz, M., 2015. Dual control of flow field heterogeneity and immobile porosity on non-Fickian transport in Berea sandstone. Water Resour. Res. 51, 8273–8293. https://doi.org/10.1002/2015WR017645.

Glover, P.W., Walker, E., 2009. Grain-size to effective pore-size transformation derived from electrokinetic theory. Geophysics 74 (1), E17–E29. https://doi.org/10.1190/1.3033217.

Grandia, F., Merino, J., Bruno, J., 2008. Assessment of the Radium-Barium Co-Precipitation and its Potential Influence on the Solubility of Ra in the Near-Field. SKB TR-08-07. Svensk Kärnbränslehantering AB (SKB), Stockholm, Sweden.

Hartikainen, J., Hartikainen, K., Hautojärvi, A., Kuoppamäki, K., Timonen, J., 1996. Helium Gas Methods for Rock Characteristics and Matrix Diffusion. Posiva-96-22. Posiva Oy, Helsinki, Finland.

Hawlicka, E., 1987. Self-diffusion of sodium, chloride and iodide ions in acetonitrile-water mixtures. J. Phys. Sci. 42, 1014–1016. https://doi.org/10.1515/zna-1987-0915.

Hellä, P., Pitkänen, P., Löfman, J., Partamies, S., Vuorinen, U., Wersin, P., 2014. Safety Case for the Disposal of Spent Nuclear Fuel at Olkiluoto: Definition of Reference and Bounding Groundwaters, Buffer and Backfill Porewaters. (Posiva Report 2014-04, Posiva Oy, Eurajoki, Finland).

Hou, X., Roos, P., 2008. Critical comparison of radiometric and mass spectrometric methods for the determination of radionuclides in environmental, biological and nuclear waste samples. Anal. Chim. Acta 608, 105–139. https://doi.org/10.1016/j.aca.2007.12.012.

Ikonen, J., Sammaljärvi, J., Siitari-Kauppi, M., Voutilainen, M., Lindberg, A., Kuva, J., Timonen, J., 2015. Investigation of Rock Matrix Retention Properties Supporting Laboratory Studies I: Mineralogy, Porosity and Pore Structure (Posiva Working Report 2014-68, Posiva Oy, Eurajoki, Finland). https://doi.org/10.1097/ANC.0000000000000232.

Ikonen, J., Sardini, P., Jokelainen, L., Siitari-Kauppi, M., Martin, A., Eikenberg, J., 2016a. The tritiated water and iodine migration in situ in Grimsel granodiorite. Part I: determination of the diffusion profiles. J. Radioanal. Nucl. Chem. 310, 1041–1048. https://doi.org/10.1007/s10967-016-4890-6.

Ikonen, J., Voutilainen, M., Söderlund, M., Jokelainen, L., Siitari-Kauppi, M., Martin, A., 2016b. Sorption and diffusion of selenium oxyanions in granitic rock. J. Contam. Hydrol. 192, 203–211. https://doi.org/10.1016/j.jconhyd.2016.08.003.

Ikonen, J., Sardini, P., Siitari-Kauppi, M., Martin, A., 2017. In situ migration of tritiated water and iodine in Grimsel granodiorite, part II: assessment of the diffusion coefficients by TDD modelling. J. Radioanal. Nucl. Chem. 311, 339–348. https://doi.org/10.1007/s10967-016-5041-9.

Iraola, A., Trinchero, P., Voutilainen, M., Gylling, B., Selroos, J.-O., Molinero, J., Svensson, U., Bosbach, D., Deissmann, G., 2017. Microtomography-based intergranular network for the simulation of radionuclide diffusion and sorption in a granitic rock. J. Contam. Hydrol. 207, 8–16. https://doi.org/10.1016/j.jconhyd.2017.10.003.

Jones, J.R., Rowlands, D.L.G., Monk, C.B., 1965. Diffusion coefficient of water in water and in some alkaline earth chloride solutions at 25°C. Trans. Faraday Soc. 61, 1384–1388. https://doi.org/10.1039/TF9656101384.

Kärki, A., Paulamäki, S., 2006. Petrology of Olkiluoto (Posiva Report 2006-02, Posiva Oy, Eurajoki, Finland). https://doi.org/10.3791/118.

Kekäläinen, P., Voutilainen, M., Poteri, A., Hölttä, P., Hautojärvi, A., Timonen, J., 2011. Solutions to and validation of matrix-diffusion models. Transp. Porous Media 87 (1), 125–149. https://doi.org/10.1007/s11242-010-9672-y.

Kuva, J., Voutilainen, M., Kekäläinen, P., Siitari-Kauppi, M., Timonen, J., Koskinen, L., 2015. Gas phase measurements of porosity, diffusion coefficient, and permeability in rock samples from Olkiluoto bedrock, Finland. Transp. Porous Media 107 (1), 187–204. https://doi.org/10.1007/s11242-014-0432-2.

Kuva, J., Sammaljärvi, J., Parkkonen, J., Siitari-Kauppi, M., Lehtonen, M., Turpeinen, T., Timonen, J., Voutilainen, M., 2018. Imaging connected porosity of crystalline rock by contrast agent-aided X-ray microtomography and scanning electron microscopy. J. Microsc. 270 (1), 98–109. https://doi.org/10.1111/jmi.12661.

Kyllönen, J., Hakanen, M., Lindberg, A., Harjula, R., Vehkamäki, M., Lehto, J., 2014. Modeling of cesium sorption on biotite using cation exchange selectivity coefficients. Radiochim. Acta 102, 919–929. https://doi.org/10.1515/ract-2013-2180.

McCarthy, J.F., 1993. Continuous-time random walks on random media. Continuous-time random walks on random media. J. Phys. A Math. Gen. 26, 2495–2503. https://doi.org/10.1088/0305-4470/26/11/004.

Molinero, J., Samper, J., 2006. Large-scale modeling of reactive solute transport in fracture zones of granitic bedrocks. J. Contam. Hydrol. 82, 293–318. https://doi.org/10.1016/j.jconhyd.2005.10.008.

Muuri, E., Ikonen, J., Matara-aho, M., Lindberg, A., Holgersson, S., Voutilainen, M., Siitari-Kauppi, M., Martin, A., 2016. Behavior of Cs in Grimsel granodiorite: sorption on main minerals and crushed rock. Radiochim. Acta 104 (8), 575–582. https://doi.org/10.1515/ract-2016-2574.

Muuri, E., Siitari-Kauppi, M., Matara-aho, M., Ikonen, J., Lindberg, A., Qian, L., Koskinen, L., 2017. Cesium sorption and diffusion on crystalline rock: Olkiluoto case study. J. Radioanal. Nucl. Chem. 311 (1), 439–446. https://doi.org/10.1007/s10967-016-5087-8.

Muuri, E., Matara-aho, M., Puhakka, E., Ikonen, J., Martin, A., Koskinen, L., Siitari-Kauppi, M., 2018. The sorption and diffusion of ^{133}Ba in crushed and intact granitic rocks from the Olkiluoto and Grimsel in-situ test sites. Appl. Geochem. 89, 138–149. https://doi.org/10.1016/j.apgeochem.2017.12.004.

Neretnieks, I., 1980. Diffusion in the rock matrix: an important factor in radionuclide retardation? J. Geophys. Res. 85, 4379–4397. https://doi.org/10.1029/JB085iB08p04379.

Nilsson, B., Papp, T., 1980. Feasibility of safe terminal disposal of spent nuclear fuel. IAEA Bull. 22 (3), 63–72.

Nilsson, K., Byegård, J., Selnert, E., Widestrand, H., Höglund, S., Gustafsson, E., 2010. Äspö Hard Rock Laboratory: Long Term Sorption Diffusion Experiment (LTDE-SD), Results from Rock Sample Analyses and Modelling. SKB R-10-68. Svensk Kärnbränslehantering AB (SKB), Stockholm, Sweden. https://doi.org/10.1016/j.sjpain.2010.05.029.

Noetinger, B., Roubinet, D., Russian, A., Le Borgne, T., Delay, F., Dentz, M., de Dreuzy, J.-R., Gouze, P., 2016. Random walk methods for modeling hydrodynamic transport in porous and fractured media from pore to reservoir scale. Transp. Porous Media 115, 345–385. https://doi.org/10.1007/s11242-016-0693-z.

Park, D.K., Ji, S.-H., 2018. Numerical simulation of anomalous observations from an in-situ long-term sorption diffusion experiment in a rock matrix. J. Hydrol. 565, 502–515. https://doi.org/10.1016/j.jhydrol.2018.08.058.

Pitkänen, P., Snellman, M., Vuorinen, U., 1996. On the Origin and Chemical Evolution of Groundwater at the Olkiluoto Site. (Posiva Report 1996-04, Posiva Oy, Eurajoki, Finland).

Posiva, 2012. Safety Case for the Disposal of Spent Nuclear Fuel at Olkiluoto—Description of the Disposal System 2012. (Posiva Report 2012-05, Posiva Oy, Eurajoki, Finland).

Posiva, 2013. Safety Case for the Disposal of Spent Nuclear Fuel at Olkiluoto – Models and Data for the Repository System 2012. (Posiva Report 2013-01, Posiva Oy, Eurajoki, Finland).

Poteri, A., Nilsson, K., Andersson, P., Siitari-Kauppi, M., Helariutta, K., Voutilainen, M., Kekäläinen, P., Ikonen, J., Sammaljärvi, J., Lindberg, A., Byegård, J., Skålberg, M., Kuva, J., Timonen, J., Koskinen, L., 2018. The First Matrix Diffusion Experiment in the Water Phase of the REPRO Project: WPDE1. (Posiva Working Report 2017-23, Posiva Oy, Eurajoki, Finland).

Puukko, E., Lehto, J., Lindberg, A., Voutilainen, M., 2018. Electromigration experiments for studying transport parameters and sorption of cesium and strontium on intact crystalline rock. J. Cantamin. Hydrol. 217, 1–7. https://doi.org/10.1016/j.jconhyd.2018.08.010.

Robinet, J.C., Sardini, P., Coelho, D., Parneix, J.C., Prêt, D., Sammartino, S., Boller, E., Altmann, S., 2012. Effects of mineral distribution at mesoscopic scale on solute diffusion in a clay-rich rock: example of the Callovo-Oxfordian mudstone (Bure, France). Water Resour. Res. 48, W05554. https://doi.org/10.1029/2011WR011352.

Sammaljärvi, J., Lindgren, A., Voutilainen, M., Kuva, J., Ikonen, J., Siitari-Kauppi, M., Pitkänen, P., Koskinen, L., 2017. Multi-scale study of the mineral porosity of veined gneiss and pegmatitic granite from Olkiluoto, Western Finland. J. Radioanal. Nucl. Chem. 314 (3), 1557–1575. https://doi.org/10.1007/s10967-017-5530-5.

Sardini, P., Delay, F., Hellmuth, K.-H., Porel, G., Oila, E., 2003. Interpretation of out-diffusion experiments on crystalline rocks using random walk modeling. J. Contam. Hydrol. 61 (1–4), 339–350. https://doi.org/10.1016/S0169-7722(02)00124-9.

Sardini, P., Robinet, J.-C., Siitari-Kauppi, M., Delay, F., Hellmuth, K.-H., 2007. Direct simulation of heterogeneous diffusion and inversion procedure applied to an out-diffusion experiment. Test case of Palmottu granite. J. Contam. Hydrol. 93 (1–4), 21–37. https://doi.org/10.1016/j.jconhyd.2007.01.011.

Smellie, J., Pitkänen, P., Koskinen, L., Aaltonen, I., Eichinger, F., Waber, N., Sahlstedt, E., Siitari-Kauppi, M., Karhu, J., Löfman, J., Poteri, A., 2014. Evolution of the Olkiluoto Site: Palaeohydrogeochemical Considerations. (Posiva Working Report 2014-27, Posiva Oy, Olkiluoto, Finland).

Soler, J.M., Landa, J., Havlova, V., Tachi, Y., Ebina, T., Sardini, P., Siitari-Kauppi, M., Eikenberg, J., Martin, A.J., 2015. Comparative modeling of an in-situ diffusion experiment in granite at the Grimsel Test Site. J. Contam. Hydrol. 179, 89–101. https://doi.org/10.1016/j.jconhyd.2015.06.002.

Tachi, Y., Yotsuji, K., Seida, Y., Yui, M., 2011. Diffusion and sorption of Cs^{+}, I^{-} and HTO in samples of the argillaceous Wakkanai Formation from the Horonobe URL, Japan: clay-based modeling approach. Geochim. Cosmochim. Acta 75, 6742–6759. https://doi.org/10.1016/j.gca.2011.08.039.

Tachi, Y., Ebina, T., Takeda, C., Saito, T., Takahashi, H., Ohuchi, Y., Martin, A., 2015. Matrix diffusion and sorption of Cs^{+}, Na^{+}, I^{-} and HTO in granodiorite: Laboratoryscale results and their extrapolation to the in situ condition. J. Contam. Hydrol. 179, 10–24. https://doi.org/10.1016/j.jconhyd.2015.05.003.

Videnská, K., Gondolli, J., Štamberg, K., Havlová, V., 2015. Retention of selenium and caesium on crystalline rock: the effect of redox conditions and mineralogical composition. J. Radioanal. Nucl. Chem. 304, 417–423. https://doi.org/10.1007/s10967-

014-3885-4.
Vilks, P., Cramer, J.J., Jensen, M., Miller, N.H., Miller, H.G., Stanchell, F.W., 2003. In situ diffusion experiment in granite: phase I. J. Contam. Hydrol. 61, 191–202. https://doi.org/10.1016/S0169-7722(02)00135-3.
Vitagliano, V., Lyons, P.A., 1956. Diffusion coefficients for aqueous solutions of sodium chloride and barium chloride. J. Am. Chem. Soc. 78, 1549–1552. https://doi.org/10.1021/ja01589a011.
Voutilainen, M., Sardini, P., Siitari-Kauppi, M., Kekäläinen, P., Aho, V., Myllys, M., Timonen, J., 2013. Diffusion of tracer in altered tonalite: experiments and simulations with heterogeneous distribution of porosity. Transp. Porous Media 96, 319–336. https://doi.org/10.1007/s11242-012-0090-1.
Voutilainen, M., Poteri, A., Helariutta, K., Siitari-Kauppi, M., Nilsson, K., Andersson, P., Byegård, J., Skålberg, M., Kekäläinen, P., Timonen, J., Lindberg, A., Pitkänen, P., Kemppainen, K., Liimatainen, J., Hautojärvi, A., Koskinen, L., 2014. In-situ experiments for investigating the retention properties of rock matrix in ONKALO, Olkiluoto, Finland. In: WM2014 Conference, March 2–6, Phoenix, Arizona, USA, https://doi.org/10.13140/2.1.2870.5924.
Voutilainen, M., Ikonen, J., Sammaljärvi, J., Kuva, J., Lindberg, A., Siitari-Kauppi, M., Koskinen, L., 2016. Through diffusion study on Olkiluoto veined gneiss and pegmatitic granite from a structural perspective. MRS Adv. 1 (61), 4041–4046. https://doi.org/10.1557/adv.2017.187.
Voutilainen, M., Kekäläinen, P., Siitari-Kauppi, M., Sardini, P., Muuri, E., Timonen, J., Martin, A., 2017. Modeling transport of cesium in Grimsel granodiorite with micrometer scale heterogeneities and dynamic update of K_d. Water Resour. Res. 53, 9245–9265. https://doi.org/10.1002/2017WR020695.
Voutilainen, M., Ikonen, J., Sammaljärvi, J., Siitari-Kauppi, M., Lindberg, A., Kuva, J., Timonen, J., Löfgren, M., 2018. Investigation of Rock Matrix Retention Properties – Supporting Laboratory Studies II: Diffusion Coefficient and Permeability (Posiva Working Report 2017-39, Posiva Oy, Eurajoki, Finland). https://doi.org/10.3389/fpsyg.2018.00530.
Voutilainen, M., Miettinen, A., Sardini, P., Parkkonen, J., Sammaljärvi, J., Gylling, B., Selroos, J.-O., Yli-Kaila, M., Koskinen, L., Siitari-Kauppi, M., 2019. Characterization of spatial porosity and mineral distribution of crystalline rock using X-ray micro computed tomography, C-14-PMMA autoradiography and scanning electron microscopy. Appl. Geochem. 101, 50–61. https://doi.org/10.1016/j.apgeochem.2018.12.024.
Wels, C., Smith, L., Vandergraaf, T.T., 1996. Influence of specific surface area on transport of sorbing solutes in fractures: an experimental analysis. Water Resour. Res. 42 (7), 1943–1954. https://doi.org/10.1029/96WR00895.
Widestrand, H., Byegård, J., Cvetkovic, V., Tullborg, E.-L., Winberg, A., Andersson, P., Siitari-Kauppi, M., 2007. Sorbing tracer experiments in a crystalline rock fracture at Äspö (Sweden): 1. Experimental setup and microscale characterization of retention properties. Water Resour. Res. 43, W10413. https://doi.org/10.1029/2006WR005277.
Widestrand, H., Byegård, J., Nilsson, K., Höglund, S., Gustafsson, E., 2010. Long Term Sorption Diffusion Experiment (LTDE-SD), Performance of Main In Situ Experiment and Results from Water Phase Measurements. SKB R-10-67. Svensk Kärnbränslehantering AB (SKB), Stockholm, Sweden.